AWARD NUMBER: W81XWH-18-1-0337

TITLE: Development of Smoothened Agonist Nonphospholipid Liposomal Nanoparticles for Bone Repair

PRINCIPAL INVESTIGATOR: Min Lee

CONTRACTING ORGANIZATION: University of California, Los Angeles, CA

REPORT DATE: November 2022

TYPE OF REPORT: Final

PREPARED FOR: U.S. Army Medical Research and Development Command
Fort Detrick, Maryland 21702-5012

REPORT DOCUMENTATION PAGE

Form Approved
OMB No. 0704-0188

1. REPORT DATE	**2. REPORT TYPE**	**3. DATES COVERED**
November 2022	Final	15Jul2018 – 14Jul2022

4. TITLE AND SUBTITLE

Development of Smoothened Agonist Nonphospholipid Liposomal Nanoparticles for Bone Repair

5a. CONTRACT NUMBER

5b. GRANT NUMBER
W81XWH-18-1-0337

5c. PROGRAM ELEMENT NUMBER

6. AUTHOR(S)
Min Lee

E-Mail: leemin@ucla.edu

5d. PROJECT NUMBER

5e. TASK NUMBER

5f. WORK UNIT NUMBER

7. PERFORMING ORGANIZATION NAME(S) AND ADDRESS(ES)
University of California, Los Angeles
10889 Wilshire Blvd Ste 700
Los Angeles CA 90095-0001

8. PERFORMING ORGANIZATION REPORT NUMBER

9. SPONSORING / MONITORING AGENCY NAME(S) AND ADDRESS(ES)

U.S. Army Medical Research and Development Command
Fort Detrick, Maryland 21702-5012

10. SPONSOR/MONITOR'S ACRONYM(S)

11. SPONSOR/MONITOR'S REPORT NUMBER(S)

12. DISTRIBUTION / AVAILABILITY STATEMENT

Approved for Public Release; Distribution Unlimited

13. SUPPLEMENTARY NOTES

14. ABSTRACT
Non-healing bone injuries represent a source of morbidity for combat casualties and military veterans, exacting both a devastating individual toll on the lives affected as well as an enormous socioeconomic burden. The manipulation of Hedgehog (Hh) signaling is a promising alternative for improved bone regeneration. In particular, the Hh activating small molecule SAG targets bone and vascular formation to induce bone healing. The present study seeks to develop a nanoparticle packaged Hh small molecule for use as a widely applicable bone graft substitute. To achieve this, we developed a novel class of liposomes formulated with single-chain amphiphiles and high content of sterols (sterosomes), resulting in significantly increased nanoparticle stability compared to conventional phospholipid. We then immobilized the sterosome onto the surface of poly (lactic-co-glycolic acid) scaffolds using dopamine intermediates to achieve controlled drug delivery in the defect site. Results showed that SAG-loaded liposomes induced a significant and dose-dependent increase in Hh-mediated osteogenic differentiation and calvarial bone healing. Favorable outcomes were achieved in comparison to standards of care, including collagen sponge delivered rBMP2 or allograft bone. This study suggests a useful nanocarrier design loading bioactive agents into functional non-phospholipid bilayers to improve clinical efficacy of current therapeutic agents.

15. SUBJECT TERMS
Non-phospholipid liposome, scaffold, smoothened agonist, hedgehog signaling, bone regeneration

16. SECURITY CLASSIFICATION OF:			**17. LIMITATION OF ABSTRACT**	**18. NUMBER OF PAGES**	**19a. NAME OF RESPONSIBLE PERSON**
a. REPORT	**b. ABSTRACT**	**c. THIS PAGE**			USAMRDC
Unclassified	Unclassified	Unclassified	Unclassified	22	**19b. TELEPHONE NUMBER** *(include area code)*

TABLE OF CONTENTS

1. INTRODUCTION

Non-healing bone injuries represent a source of morbidity for combat casualties and military veterans, exacting both a devastating individual toll on the lives affected as well as an enormous socioeconomic burden. The manipulation of Hedgehog (Hh) signaling is a promising alternative for improved bone regeneration. Our research group has shown that Hh signaling diverts mesenchymal stem cells (MSC) toward a bone-forming fate and away from competing cell fates. Moreover, the Hh activating small molecule SAG targets bone and vascular formation to induce bone healing. In a coordinate research effort, we have shown that non-phospholipid liposomes composed of Stearylamine and Oxysterol (SA/Oxy) have intrinsic bone inducing capabilities, and are well designed to deliver the small molecule SAG to sites of bone injury. In aggregate, the present proposal seeks to develop a nanoparticle (NP) delivered small molecule for faster, safer, and more efficacious bone repair than currently available treatment strategies. Here, we will perform key preclinical safety and efficacy studies for clinical translation of a nanoparticle packaged Hh small molecule for use as a widely applicable bone graft substitute, to be accomplished in two specific aims.

2. KEYWORDS

Non-phospholipid liposome, scaffold, smoothened agonist, hedgehog signaling, bone regeneration

3. ACCOMPLISHMENTS

What were the major goals of the project?

The project contains two aims as stated in the SOW:

Aim 1: Optimize SAG-loaded liposomal nanoparticles for mouse calvarial defect repair.
Aim 2: Determine the safety of SAG-loaded liposomal nanoparticles for mouse calvarial defect repair.

These aims are composed of two subtasks:

Subtask 1: Osteoinductive scaffold fabrication and batch validation
Subtask 2: SA/Oxy NP production and batch validation

What was accomplished under these goals?

- Develop SAG-loaded Oxysterol (Oxy) liposomes and validate bioactivity

Oxy liposomes were prepared by self-assembly of SA and 20S-Oxy using thin film hydration technique. **Table 1** shows the hydrodynamic size, polydispersity index (PDI), ζ-potentials, and loading efficiency of the liposomes. The size distribution of Oxy liposomes was 142.5 ± 4.9 nm for Oxy liposomes and 145.4 ± 2.7 nm for SAG-loaded Oxy liposomes (SAG-Oxy liposome) with approximately 0.2 of PDI (**Figure 1A**). The ζ-potentials of both liposomes were highly positive, around 55-60 mV.

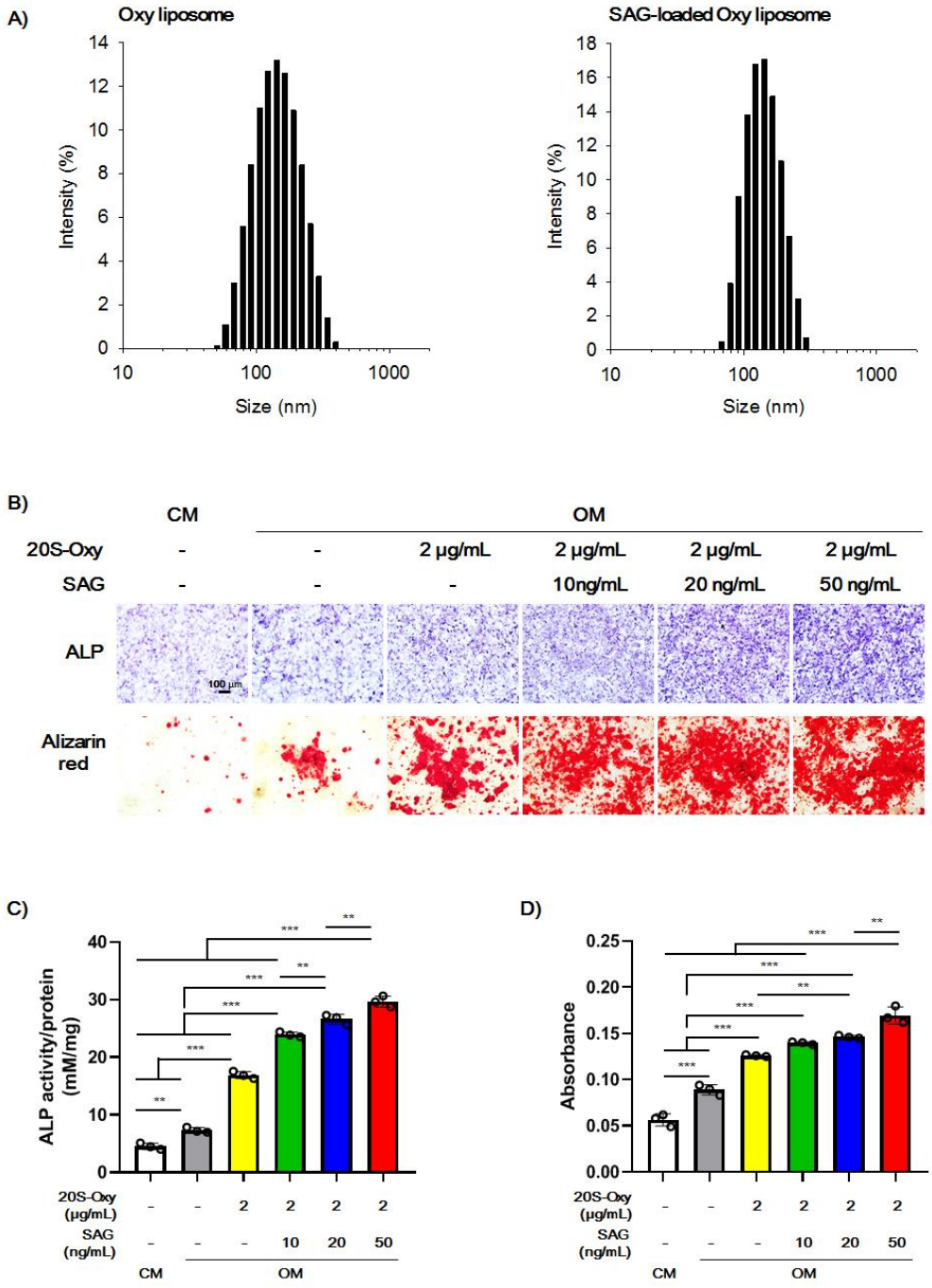

Figure 1. Characterization of Oxysterol (Oxy) liposomes. **A**) Size distributions of Oxy liposomes and Smoothened Agonist (SAG)-loaded Oxy liposomes. (**B**, upper line) Alkaline phosphatase (ALP) staining and **C**) colorimetric quantification of ALP activity at day 4 of osteogenic differentiation. (**B**, bottom line) Mineralization stained with Alizarin red S and **D**) colorimetric quantification of mineralization activity at day 14 of differentiation. Scale bars are 200 μm. All data were presented as means ± SD. $^{**}P < 0.01$, $^{***}P < 0.001$ as determined using a one-way ANOVA with Tukey's post hoc test. CM = Culture medium, OM = Osteogenic medium.

Table 1. Characterization of Oxy liposomes and SAG-loaded Oxy liposomes.

	Oxy liposome	**SAG-loaded Oxy liposome**
Appearance	Clear	Clear
Size (nm)	142.5 ± 4.9	145.4 ± 2.7
PDI	0.231 ± 0.042	0.154 ± 0.028
Zeta potential (mV)	60.3 ± 3.5	55.9 ± 1.2
Loading efficiency	-	52.6 ± 2.9 %

ALP, an early stage marker of osteogenic differentiation, was assessed at day 4 of differentiation. The Oxy liposomes without SAG-loading induced ALP expression compared to non-treated groups (**Figure 1B**, upper panels). The ALP staining synergistically intensified with SAG-loading and demonstrated a dose-dependent increase with ascending SAG content. A quantitative analysis of ALP expression confirmed this finding, with ascending SAG-loading concentrations leading to a dose-dependent 3.7- to 6.6-fold increase in comparison to culture medium (CM) (**Figure 1C**). Alizarin red S (ARS) staining was further carried out to determine matrix mineralization (**Figure 1B**, bottom panels). Similar to ALP expression, more intense mineral deposition was observed in Oxy liposome-treated groups. Furthermore, SAG-Oxy liposomes induced a dose dependent increase in mineralization. Photometric quantification of ARS confirmed these results (**Figure 1D**), with mineralization was increased up to 3.0-fold in SAG-Oxy liposome treatment groups.

- Combine SAG-loaded Oxy liposome with 3D PLGA scaffolds

Oxy liposome-coated scaffolds were fabricated by a series of coating with polydopamine (pD) substrate and Oxy liposome as follows: Apatite-PLGA was coated by sequential incubation in pD solution, Oxy liposome solution, and pD solution. Scanning electron microscopy (SEM) was used to characterize the microstructure of scaffolds (**Figure 2A**). All the scaffolds showed the typical porous structure with highly interconnected about 200-300 μm pore size, whereas PLGA scaffold prior to any modification displayed a flat strut surface. Apatite-PLGA scaffolds upon immersion in stimulated body fluid (SBF) were fabricated with nubby textured structures on the surface along the strut. After the serial functionalization with pD, and Oxy liposome on the scaffold, there was no obvious change in microstructure morphology of PLGA and Apatite-PLGA.

The scaffolds were further analyzed by energy dispersive X-ray spectroscopy (EDX) to uncover the engineered surfaces (**Figure 2B**). The spectra showed that the chemical composition of the surfaces was dramatically altered by the apatite-coating, resulting in new peaks for calcium (Ca) and phosphorus (P), which was close to the theoretical Ca/P ratio of HA (**Figure 2C)**. After functionalization with pD and Oxy liposome, the atomic composition of both Ca and P was subsequently decreased due to the cover with the carbon-rich layers of pD and Oxy liposomes.

Next, we evaluated the pD-mediated functionalizing efficacy of Oxy liposomes onto the scaffold surface using nile red-loaded Oxy liposomes, of which nile red was used as a fluorescence model drug (**Figure 2D**). There were intense red fluorescence signals on pD-coated Apatite-PLGA scaffolds after coating with nile red-loaded Oxy liposomes. However, the signals were extremely

low on Apatite-PLGA scaffolds without a pD layer. Furthermore, the coating amount of Oxy liposome could be managed by controlling reaction time and concentration of the liposome (**Figure 2E**).

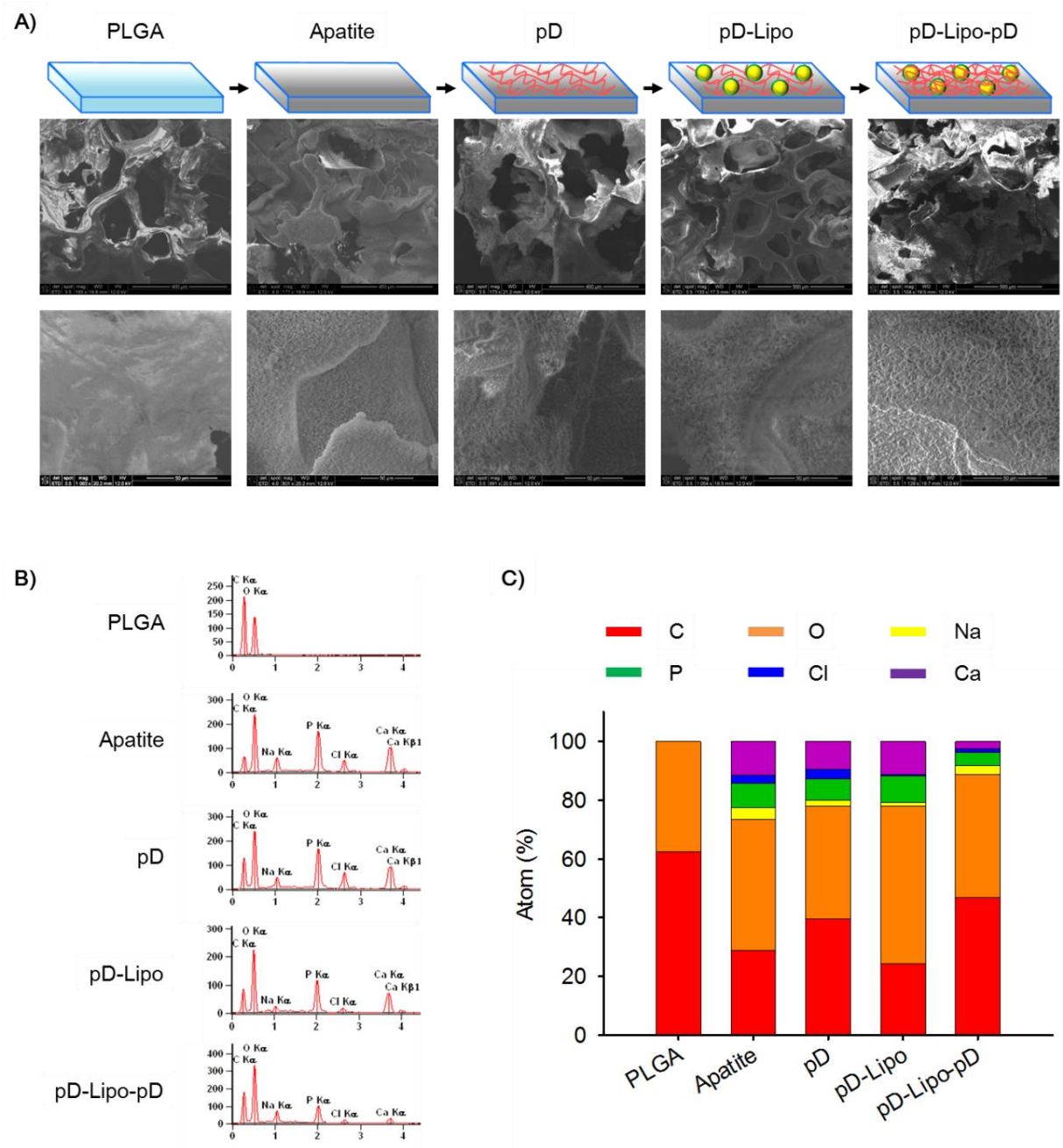

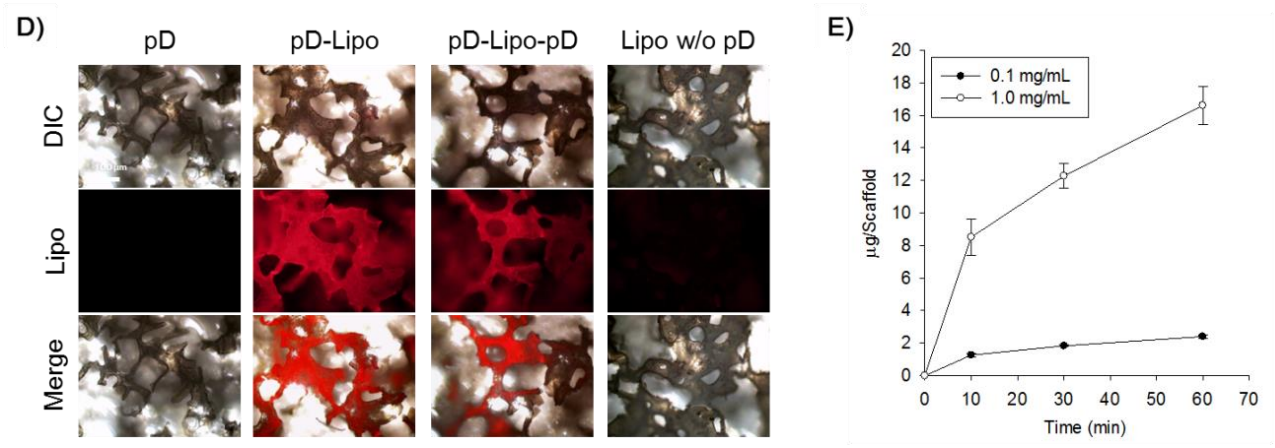

Figure 2. Characterization of PLGA scaffolds with Oxysterol (Oxy) liposomes. **A**) Scanning electron microscopy (SEM) images and **B**) EDX spectra of PLGA, Apatite-coated PLGA (Apatite-PLGA), pD-coated Apatite-PLGA, pD-Lipo-coated Apatite-PLGA, and pD-Lipo-pD-coated Apatite-PLGA scaffolds. **C**) Elemental composition of the scaffold surface, determined by EDX. **D**) Fluorescence microscopy images of Oxy liposome on Apatite-PLGA scaffolds in the presence or absence of pD layer. Nile red was used as a model cargo. **E**) Quantification of Oxy liposomes on surface of pD-coated scaffold for 1 h. Nile red-loaded Oxy liposome was used as a model liposome. Data were presented as mean ± SD. PLGA = Poly(lactic-co-glycolic acid), Lipo = Oxy liposome, pD = Polydopamine.

- Evaluate bioactivity of liposome-immobilized scaffolds

To evaluate the biocompatibility of the Oxy liposome-engineered scaffolds, we seeded mouse BMSCs onto the 3D porous scaffolds with various surfaces and allowed them to adhere for 4 h, followed by further incubation in culture medium for 7 days. No toxic effect of the pD-functionalization was observed as evidenced by consistent metabolic activity in Alamar Blue assay (**Figure 3A**) and high viability with Live/Dead staining (**Figure 3B**). The metabolic activity also showed that the seeded cells proliferated with no significant differences over time in all groups except for Oxy liposome-coated scaffolds without additional pD-coating. Even though the toxicity of Oxy liposome-coated scaffold without additional pD-coating was detected in both assay and staining, the cytocompatibility was recovered and the cells demonstrated adherence with the additional pD layer. Live/dead staining after 7 day culture demonstrated that the seeded cells were viable and uniformly adherent to the functionalized scaffolds, with the exception of Oxy liposome-coated scaffolds without additional pD-coating.

Following the investigation of biocompatibility on the scaffolds, we turned to evaluate the osteogenic capacity and the regulation of Hh signaling of Oxy liposome-coated scaffolds toward BMSCs at the molecular level. The quantitative real-time polymerase chain reaction (qRT-PCR) result revealed that the expression levels of osteogenic markers including *ALP*, *Runx2*, and *OCN* in cells seeded on the Oxy liposome-coated scaffolds were upregulated by 19.8-, 2.2-, and 2.1-fold, respectively, compared with those in cells seeded in the Apatite-PLGA scaffolds without Oxy liposomes (**Figure 3C**, **D**, and **E**). In particular, the scaffolds with SAG-loading led to much greater influence on the expression levels of these osteogenic genes compared with corresponding levels in

the other groups (Apatite-, pD, and Oxy liposome-coated scaffolds). The scaffolds with the highest SAG contents (Oxy liposome +45 ug/mL SAG) showed increased expressions of all osteogenic markers.

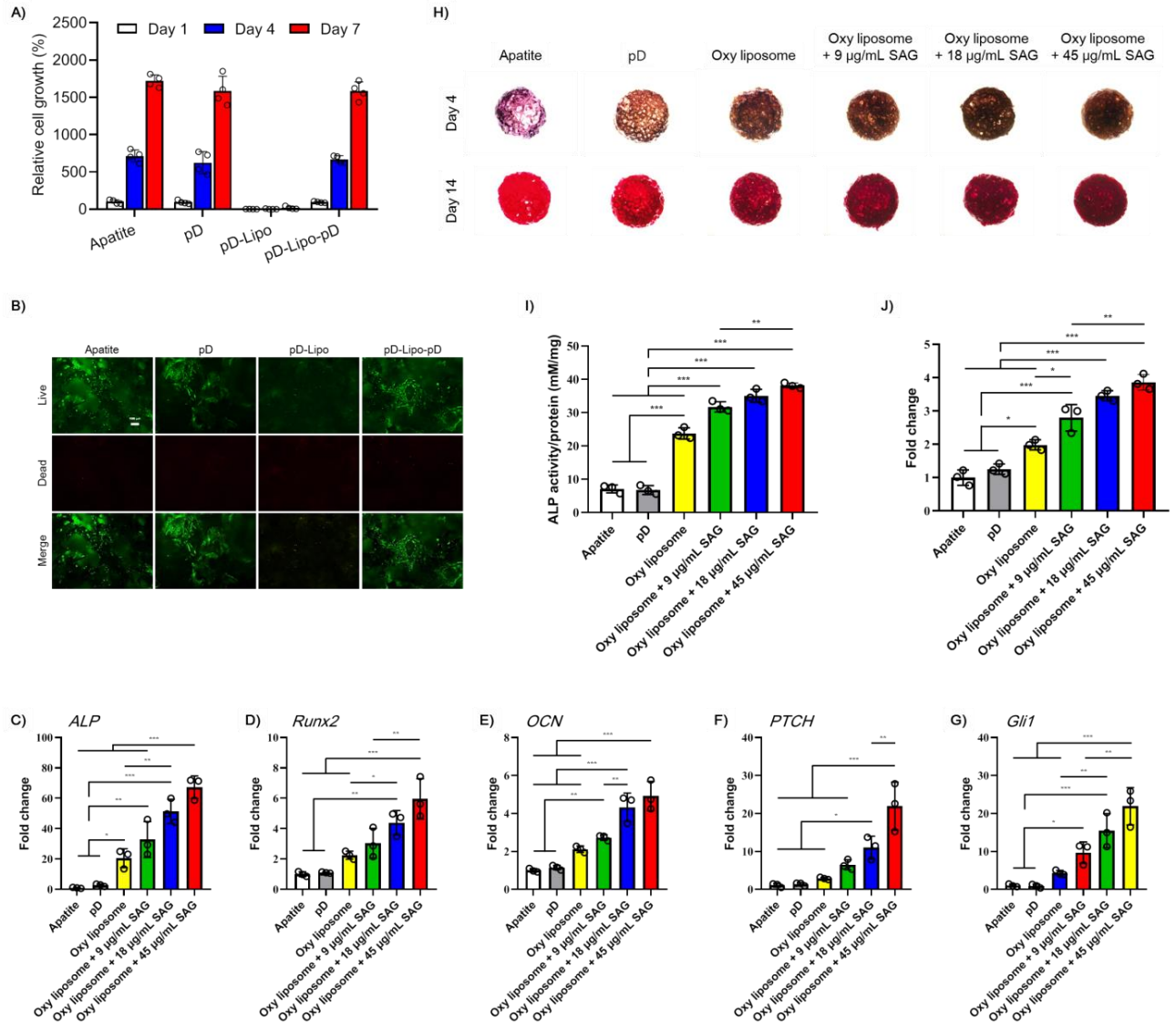

Figure 3. Cell adherence, proliferation, and bioactivity evaluations of SAG-loaded Oxysterol (Oxy) liposome-coated scaffolds. **A**) *In vitro* cell proliferation after 1, 4, and 7 days. The value was normalized by Apatite-PLGA scaffold of day 1. **B**) Representative fluorescence images of BMSCs stained with calcein AM (live cells, green fluorescence) and ethidium homodimer (dead cells, red fluorescence), day 7. Scale bar is 200 μm. **(C-G)** Gene expression related to osteogenesis and Hh signaling pathway. **C**) *ALP*, **D**) *Runx2*, **E**) *OCN*, **F**) *PTCH*, and **G**) *Gli1* were evaluated after 7 d incubation. **H**, top line) ALP staining and **I**) colorimetric quantification of ALP activity at day 4. **H**, bottom line) Mineralization stained with Alizarin red S and **J**) colorimetric quantification of mineralization activity at day 14. All data were presented as means ± SD. $^{**}P < 0.05$, $^{**}P < 0.01$,

***$P < 0.001$ as determined using a one-way ANOVA with Tukey's post hoc test. ALP = Alkaline phosphatase, Runx2 = Runt-related transcription factor 2, OCN = Osteocalcin, PTCH = Protein patched homolog 1, Gli1 = GLI Family Zinc Finger 1.

Next, we assessed Hh pathway signaling activation in cells seeded on the scaffolds by qRT-PCR (**Figure 3F** and **G**). The Hh pathway markers, *Ptch1* and *Gli1*, were upregulated by Oxy liposome coating on the scaffolds, although there are no significant differences. The levels of these genes expression were significantly increased among SAG-Oxy liposomes treated scaffolds, and showed a dose-dependent increase with SAG content.

We also examined the osteoinductive effect of Oxy liposome-coated 3D porous scaffolds, when seeded with BMSC and cultured in osteogenic medium. Consistent with the results of qRT-PCR, more intense ALP staining was observed in Oxy liposome-coated scaffolds compared to the control groups at day 4 (**Figure 3H**, top panels). Moreover, the level of ALP staining was gradually increased with ascending content of SAG-loading. Quantitative analysis of ALP activity confirmed this impression, demonstrating a significant increase not only between the Oxy liposome-coated scaffolds and the control groups, but also between Oxy liposome- and SAG-loaded Oxy liposome-coated scaffolds (**Figure 3I**). ARS staining (**Figure 3H**, bottom panels) further analyzed the accumulation of mineralized matrix during osteogenic differentiation of BMSCs. The results showed that the deposition of mineralized matrix was markedly enhanced in Oxy liposome-coated scaffolds, and further intensified with SAG-loading into Oxy liposomes (**Figure 3J**).

- Evaluate *in vivo* efficacy of SAG-loaded SA/Oxy nanoparticles

SAG-loaded liposomal nanoparticles were immobilized onto trabecular bone-mimetic apatite-coated 3D scaffolds using bio-inspired polydopamine adhesives to ensure favorable microenvironments for cell growth and local drug delivery. The scaffolds integrated with SAG-loaded Oxy liposome were evaluated for bone-forming efficacy using a parietal bone defect model in adult mice (**Figure 4**). Progressive bone defect healing was evaluated over an 8 week period. Micro-CT analysis was performed, and reconstructions visualized either as coronal crossections or from a top down perspective (**Figure 4A-F**). As expected, untreated "empty" defects or polydopamine (pD) treated scaffolds showed minimal new bone formation. A modest osteoinductive effect was observed with Oxy liposome laden scaffolds. In contrast, significant and dose-dependent re-ossification was observed with SAG loaded Oxy liposome scaffolds.

Quantitative micro-CT analysis confirmed these findings. Bone volume **(Figure 4G)** and Bone volume density **(Figure 4H)** analysis a significant a dose-dependent increase with 18 or 45 ug/mL SAG loading. In agreement with these findings, bone surface **(Figure 4I)** and bone perimeter **(Figure 4J)** analysis also showed a significant increase among SAG loaded Oxy liposome scaffolds, particularly at the highest dose.

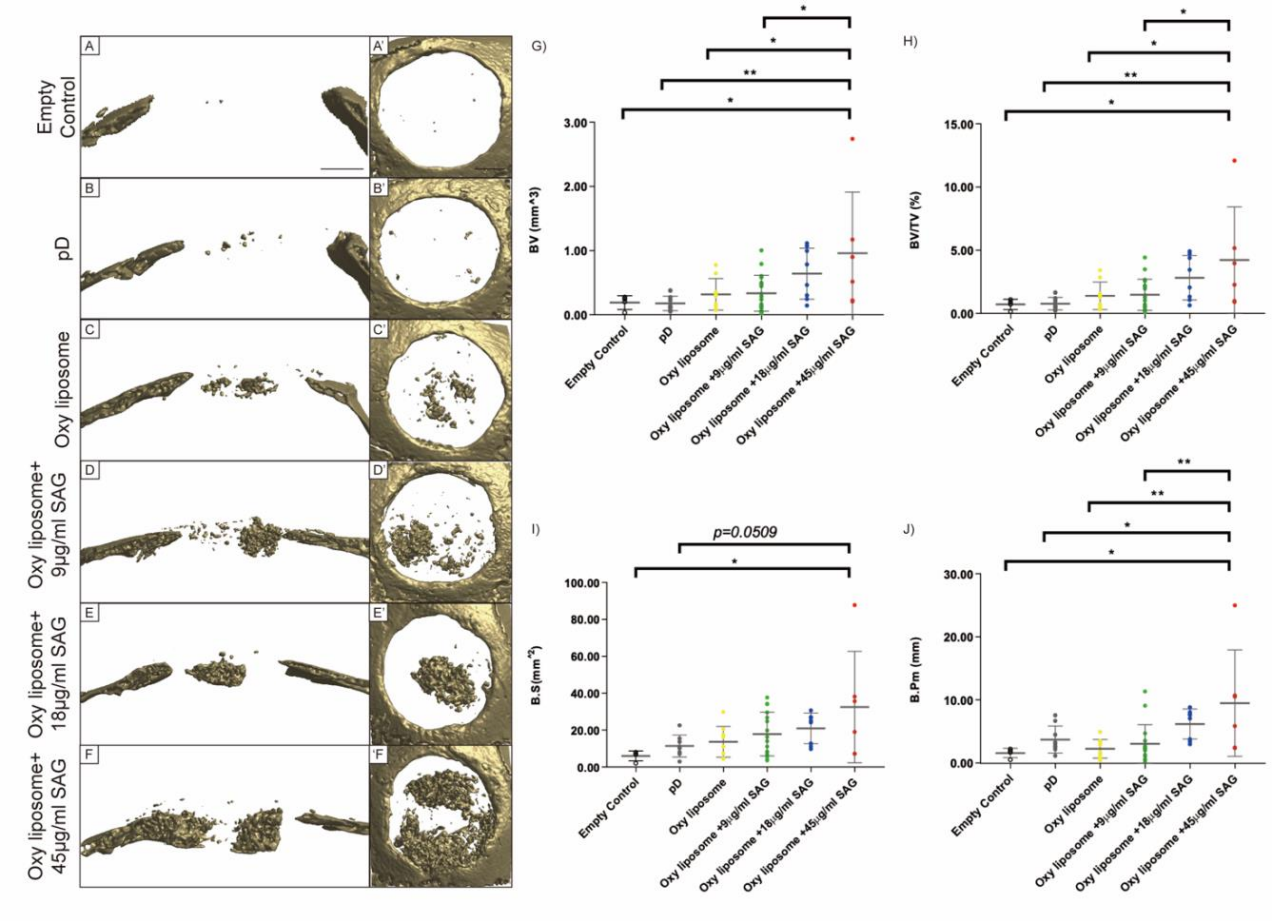

Figure 4. Micro-CT analysis of calvarial healing induced by SAG-loaded Oxy liposome-coated scaffolds. **A-F)** Representative 3D micro-CT reconstructions of calvarial defect site, shown in coronal section or **A'-F')** top-down view, 8 weeks after implantation. **G-J)** Micro-CT quantification of bone regeneration in calvarial defects. A 4 mm diameter cylindrical volume-of-interest (VOI) was used. Quantification of bone regeneration including **G)** Bone volume (BV), **H)** Bone volume density (bone volume per tissue volume, BV/TV), **I)** Bone surface (B.S) and **J)** Bone perimeter (B.Pm). The pD, and Oxy liposome groups are pD-coated Apatite-PLGA scaffolds, and pD-Oxy liposome-pD-coated Apatite-PLGA scaffolds, respectively. Data presents as mean ± SD with each dots representing an individual animal (n=4~18). *$p < 0.05$; **$p < 0.01$, as determined using a one-way ANOVA with Tukey's post hoc test. Scale bar = 1 mm.

- Comparison to BMP2 or allograft bone

The previously optimized Oxy liposome +45 ug/mL SAG formulation was next compared with two common methods of bone defect repair, including recombinant BMP2 or decellularized allograft bone. BMP2 loaded collagen sponge was used at clinical dosages of 1.5 mg/ml. Decellularized calvarial bone from a syngeneic adult mice was trimmed to exactly fit the defect size and placed in the calvarial defect without additional treatment. By 3D micro-CT reconstructions and histomorphometry, BMP2 treated defect showed overgrowth and porous bone while the allograft showed essentially no incorporation with native bone (**Figure 5A-C**).

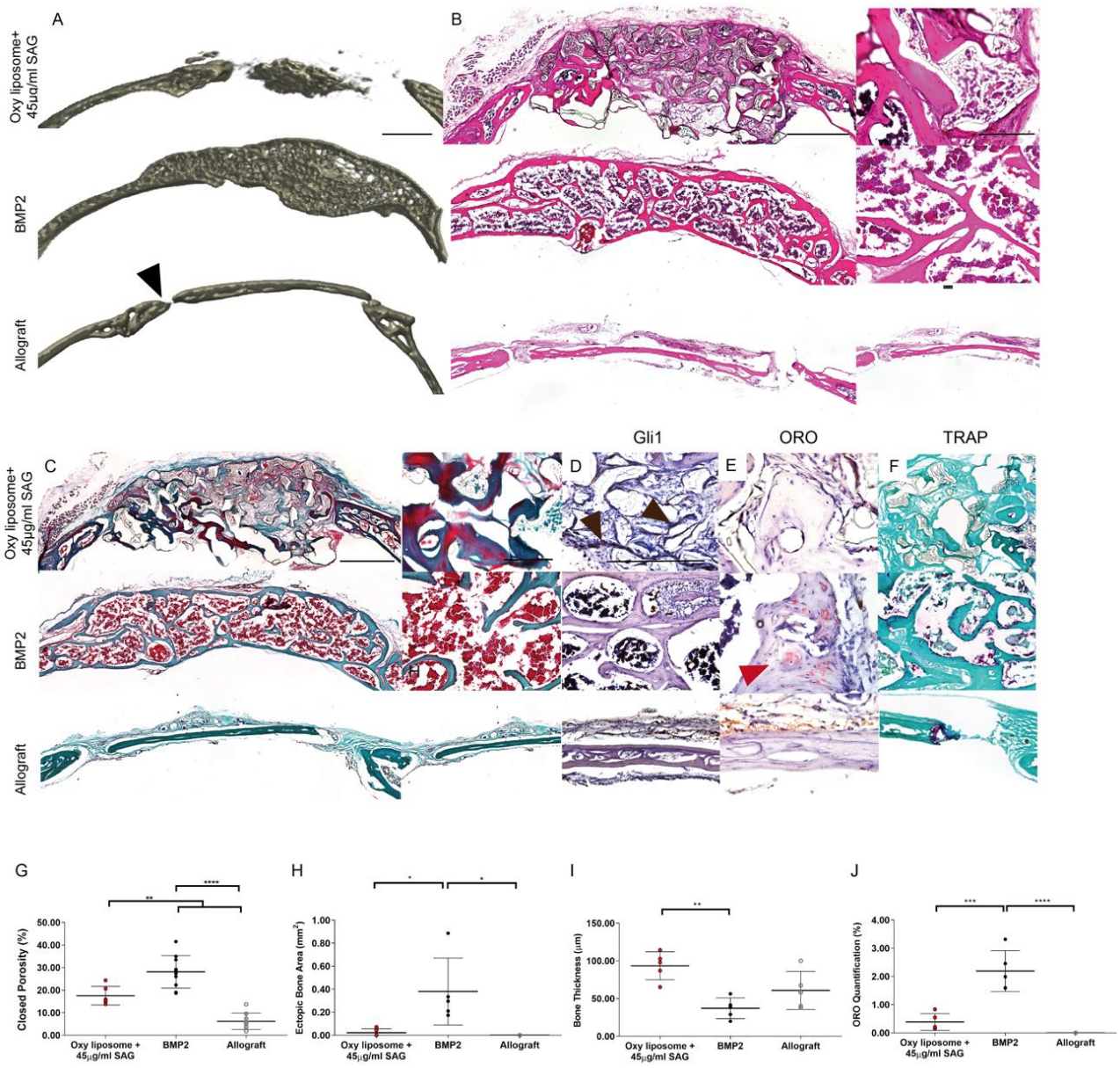

Figure 5. Histologic analysis of calvarial healing induced by SAG-loaded Oxy liposome-coated scaffolds in comparison to BMP2 or decellularized allograft. **A)** Representative 3D micro-CT reconstructions of calvarial defect site, shown in coronal section **B)** Representative H&E staining (right), **C)** Goldner's Trichrome staining (left), and corresponding high magnification images staining of **D)** Gli1 immunohistochemistry, **E)** Oil Red O histochemical staining and **F)** TRAP histochemical staining among coronal cross-sections of the calvarial defect, 8 weeks after implantation. **G)** Micro-CT quantification of closed porosity in calvarial defects. Histomorphometric analyses including **H)** Ectopic Bone Area, **I)** Bone Thickness and **J)** Oil Red O Quantification. Data presents as mean ± SD (n=5~8). *$p < 0.05$; **$p < 0.01$; ****$p < 0.0001$, as determined using a one-way ANOVA with Tukey's post hoc test. Scale bar: 1 mm in tile scans and 0.5 mm in high magnification images. Gli1=GLI family zinc finger 1, ORO=Oil Red O, TRAP=Tartrate-resistant acidic phosphatase.

As expected, the target Hh protein Gli1 showed induction among Oxy liposome +45 ug/mL SAG treated defects, while treatment with BMP2 or allograft bone did not induce high Gli1 expression by immunohistochemistry (**Figure 5D**). Interestingly, Oil red O staining showed increased accumulation of lipid within the defect site among BMP2 treated samples, reflecting inappropriate adipogenesis (**Figure 5E)**. No increase in lipid accumulation was noted in either Oxy liposome +45 ug/mL SAG treated defects nor allograft treated injury sites (**Figure 5E**). Assessments of inflammation were performed using immunohistochemical staining for the macrophage marker CD68 (data now shown). Inconspicuous macrophages were detected in Oxy liposome +45 ug/mL treated defects. In contrast, BMP2 treated defects showed high overall immunoreactivity for CD68. Finally, osteoclast numbers were assessed by TRAP staining (**Figure 5F**). An increase in TRAP+ cells was apparent in BMP2 treated defects only. Across sections, decellularized allograft bone showed little new bone formation. 3D micro-CT renderings and histology demonstrated little if any osseous incorporation into the native bone (black arrowhead, **Figure 5A-C**).

Quantitative analysis was performed which reflected these findings. Micro-CT analysis demonstrated increased porosity among BMP2 treated defects (**Figure 5G**), and likewise histomorphometric analysis showed increased ectopic bone formation induced by BMP2 (**Figure 5H**). In contrast, Oxy liposome +45 ug/mL SAG treated defects showed conspicuously increased thickness of bone trabeculae in comparison to other treatments (**Figure 5I**). Finally, quantitative analysis of Oil red O staining showed increased lipid droplets in newly formed bone within BMP2 treated defects (**Figure 5J**).

- Preparation of bone-targeting exosome mimetics (EMs)

Exosomes secreted by MSCs are currently being explored for use in tissue engineering and regenerative medicine. A new approach of generating exosome-mimetic nanovesicles has been introduced by mechanically disrupting plasma membranes of cells and re-assembling the contents into nanovesicles (**Figure 6**). The potential of an extracellular vesicle system as a carrier for SAG was examined by isolating EMs from MSCs.

Click chemistry was utilized to conjugate bone targeting ligand, alendronate (ALN), onto EM surface. In brief, 1) reactive azide groups were displayed on the cell surface by a metabolic engineering technique, which introduces unnatural glycans on the cell surface by feeding specific precursors (tetraacetylated N-azidoacetyl-D-mannosamine, Ac_4ManNAz) through their intrinsic metabolism. 2) Azide-displayed EM (N3-EM) was fabricated by sequential extrusion and purification as described above. 3) ALN was functionalized with DBCO and coupled onto the EM surface via click crosslinking reaction between the azides (on EM) and DBCO groups (on ALN).

Dynamic light scattering served to measure the particle size, zeta potential, and polydispersity index (PDI) of the EMs. The hydrodynamic diameter of the EMs was around 20-80 nm, with a narrow distribution (PDI $\leq$ 0.3) and no significant differences. The ζ-potential for all types of EMs with or without chemical modifications was negative, approximately -25 mV. No significant changes occurred after the serial metabolic and bioorthogonal surface engineering on the EMs.

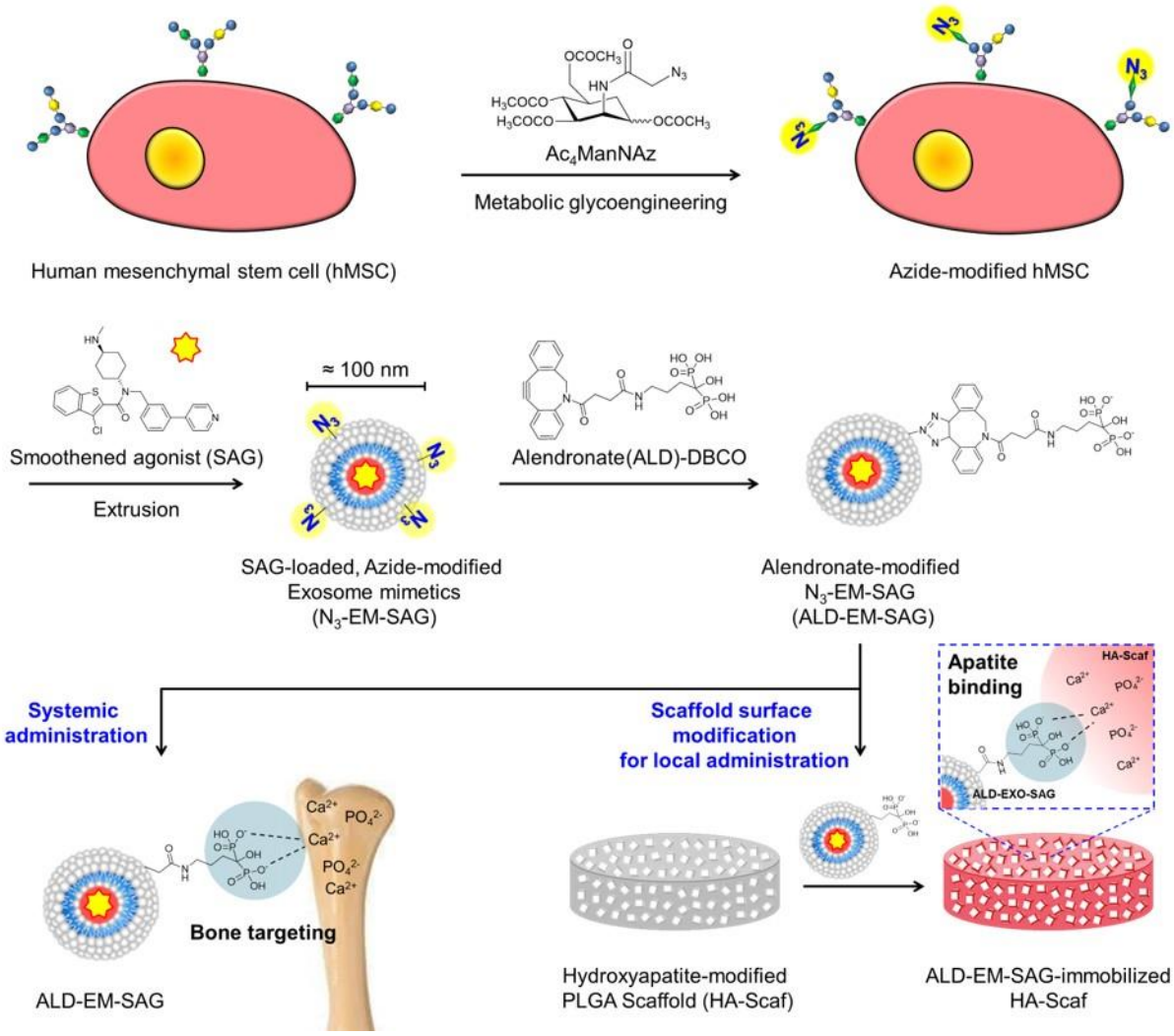

Figure 6. Schematic illustration of bone-targeting exosome mimetics (EMs) engineered through bioorthogonal surface functionalization for bone regeneration. The azides are generated on the surface of cells through metabolic glycoengineering. The drug (Smoothened agonist, SAG)-loaded EMs are fabricated by means of an extrusion method. Bone-targeting ligands (alendronate, ALD) are attached to the azides on the surface of EMs through bioorthogonal click chemistry. The resulting EMs (ALD-EM-SAG) can accomplish bone-targeting drug delivery and the surface engineering of biomaterial scaffolds for systemic and local bone regeneration.

- Binding affinity of EMs to bone mineral

Bone binding ability of ALN-EM was determined by hydroxyapatite (HA) or *ex-vivo* bone binding assay using fluorescence Dil-labeled EM. Strong binding of ALN-EM to HA-coated 3D PLGA scaffolds was evidenced by a remarkable increase of fluorescence vs. unmodified or azide-modified exosomes (EM or N3-EM) (**Figure 7B**). In addition, the binding efficiency of ALN-EM toward HA-PLGA was increased up to 85% after 48 h, whereas EM and N3-EM showed low HA binding of 40% with non-specific adsorption (**Figure 7C**). We observed a typical porous morphology with a pore size of around 200-300 μm and a highly interconnected structure in all of the scaffolds (**Figure**

7D). EDX spectra showed peaks for calcium (Ca) and phosphorus (P) corresponding to HA layers. Lastly, bone affinity of ALN-EM was determined by *ex vivo* bone binding assay in mouse calvaria (**Figure 7E**). Fluorescence microscopy demonstrated a significant rise in the bone binding of ALN-EM, while non-targeted EM (N3-EM) showed no specific binding to bone fragments.

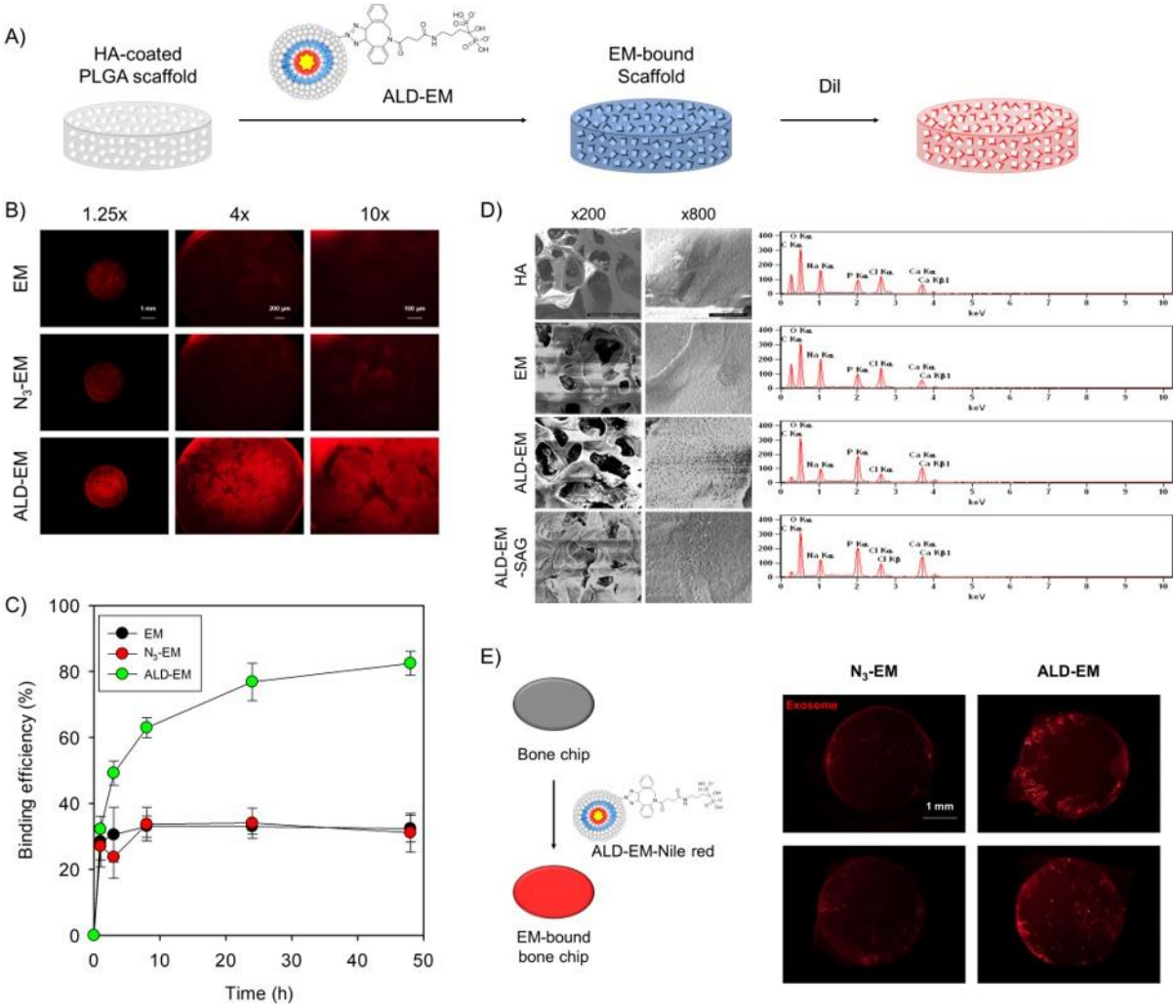

Figure 7. Binding ability of bone-targeting exosome mimetics on the HA-coated PLGA scaffold and mouse skull bone (*ex vivo*). A) Schematic illustration of the bone-binding experiment with the HA-coated PLGA scaffold. B) Fluorescence images of EM-bound PLGA scaffolds after incubating for 24 h and staining with Dil dye. C) The binding kinetics of various EMs to the HA surface at various incubating times (means ± standard deviation, n = 3). D) SEM images and EDX spectra of various surfaces (HA, EM, ALD-EM, and ALD-EM-SAG). The scale bar indicates 400 and 50 μm for low and high magnification images, respectively. E) Schematic illustration of *ex vivo* bone-binding experiment with a mouse skull bone chip with nile red-loaded ALD-EXOs and fluorescence images of EM-bound bone chips.

- Bioactivity of SAG/EMs bound hybrid scaffolds

We demonstrated the bone repair capacity of the hybrid scaffolds in a critical-sized mouse calvarial defect model. We evaluated three types of scaffolds, including bare scaffolds and EM-bound scaffolds in the presence or absence of SAG, in parallel for comparison. The microCT scanning and quantitative analysis were performed 12 weeks post-implantation to evaluate the bone regeneration capability. A representative 3D reconstructed image of the defect area showed substantially greater regeneration of new bone after the implantation of the scaffolds with EMs compared to control groups (**Figure 8A**). Notably, the EM-bound hybrid scaffold with SAG delivery led to the most effective bone repair with the greatest coverage of the defect site. (**Figure 8B**). Quantitative analyses of the microCT results (BV/TV, bone mineral density, and trabecular number) suggest that the EM-engineered hybrid scaffold exhibits excellent performance in the re-ossification of bone defects where EMs can act as an effective osteogenic activator and delivery vector for SAG (**Figure 8C**).

Histological evaluations by H&E, Masson's trichrome, and Picrosirius red staining also support the radiographic results (**Figure 8F**). We also conducted immunohistochemical staining of Runx2 and OCN as osteogenic markers to assess the extent of reossification (**Figure 8G**). We observed strong positive staining for both the Runx2 and OCN staining in the osteoblasts and osteocytes along the regenerated bone area in the SAG-containing EM-bound hybrid scaffold. This result indicates that the biomaterial scaffold with EM application and stimulation by SAG delivery promotes the osteoinductive capacity for efficacious bone healing.

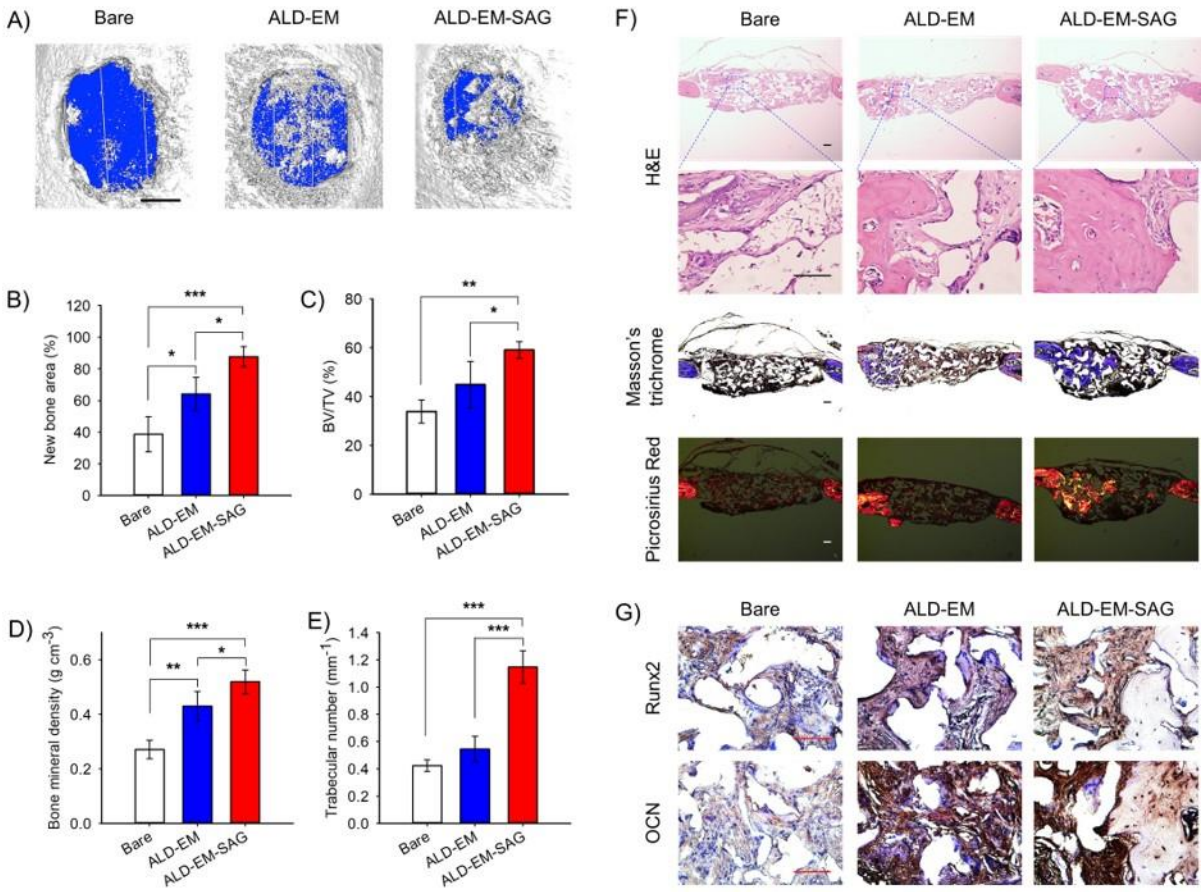

Figure 8. Effect of bone regeneration *in vivo* on calvarial defect following the implantation of EM-bound scaffolds. A) Representative 3D reconstructed images of calvarial defect 12 weeks after the implantation of EM- or SAG-loaded EM (EM-SAG)-bound scaffolds taken with superficial view. The scale bar represents 1 mm in A). The quantified parameters of the regenerated bone, including B) new bone area, C) bone volume density (BV/TV; bone volume: BV; tissue volume: TV), D) bone mineral density, and E) trabecular number taken at the 3 mm diameter cylindrical defect. All data are presented as mean ± SD (n= 4). The statistical analyses were done with one-way ANOVA with Tukey's post hoc test; *$p< 0.05$, **$p< 0.01$, and ***$p< 0.001$. F) Histologic sections of calvarial decalcified sections stained with H&E, Masson's trichrome, and Picrosirius red after 12 weeks of implantation. G) Immunohistochemical analysis of Runt-related transcription factor 2 (Runx2) and Osteocalcin (OCN) after 12 weeks of implantation. The scale bars indicate 100 μm in F) and G).

Key outcomes and conclusions:

SAG was successfully encapsulated into Oxy liposomes and its bioactive and osteogenic potential was verified before progression to scaffold loading and *in vivo* application.

SAG-loaded Oxy liposomes were successfully integrated with PLGA scaffolds using bio-inspired polydopamine adhesives and induced a significant and dose-dependent increase in Hh-mediated osteogenic differentiation.

SAG-loaded Oxy liposomes on a bio-inspired scaffold led to osseous healing of critical size bone defects in mice, demonstrating the potency of nanoparticle packaged SAG.

SAG-loaded liposomes induced more robust bone defect repair compared to standards of care, including collagen sponge delivered rBMP2 or allograft bone, demonstrating their potential advantages over current products.

Given the potential cytotoxicity of Oxy liposomes associated with its strong cationic nature, cell-derived extracellular vesicles were explored as an alternative vector to deliver SAG in a more efficient and safer manner.

What opportunities for training and professional development has the project provided?

This project provided a number of opportunities for the postdoctoral participants to learn various drug delivery techniques and acquire in-depth knowledge of signaling molecules and mechanisms involved in bone regeneration.

How were the results disseminated to communities of interest?

Our novel findings have been disseminated by publication in scientific journals.

What do you plan to do during the next reporting period to accomplish the goals?

N/A

4. IMPACT

What was the impact on the development of the principal discipline(s) of the project?

This study developed a novel class of liposomes composed of non-phospholipid molecules formulated with single-chain amphiphiles and high content of sterols (sterosomes). The high sterol content in our sterosomes induces well-ordered lipid bilayer chains with very limited permeability and significantly increased nanoparticle stability compared to conventional phospholipid. This system can be advantageous for delivery of small molecular drugs or other therapeutic genes. Liposomes are generally made from pharmacologically inactive substances. Oxysterols used in this study are interesting sterol molecules for applications targeting damaged bone treatment. Including oxysterol into our liposomal formulation not only increased nanoparticle stability but also stimulated cells to develop into bone-forming cells. We combined this breakthrough to develop a hybrid scaffold as a bone graft substitute product by covalently immobilizing drug-loaded liposomes onto three dimensional scaffolds via a bio-inspired polydopamine intermediate without complicated chemical modification. Favorable outcomes were achieved in comparison to standards of care, including collagen sponge delivered rBMP2 or allograft bone. We also employed cell-derived extracellular vesicles as an alternative delivery vector for SAG. This is the first demonstration of a hedgehog agonist bone graft device for faster and more efficacious bone repair. The additional knowledge gained from this study may suggest nanocarrier design strategies loading bioactive agents into functional non-phospholipid bilayers or exosomal biovectors to improve clinical efficacy of current therapeutic agents.

What was the impact on other disciplines?

Nothing to Report

What was the impact on technology transfer?

Nothing to Report

What was the impact on society beyond science and technology?

Nothing to Report

5. CHANGES/PROBLEMS

Changes in approach and reasons for change

Nothing to Report

Actual or anticipated problems or delays and actions or plans to resolve them

Nothing to Report

Changes that had a significant impact on expenditures

Nothing to Report

Significant changes in use or care of human subjects, vertebrate animals, biohazards, and/or select agents

Nothing to Report

6. PRODUCTS

- **Publications, conference papers, and presentations**

Journal publications.

1. Lee CS, Kim S, Fan J, Hwang HS, Aghaloo T, Lee M. Smoothened Agonist Sterosome Immobilized Hybrid Scaffold for Bone Regeneration. Science Advances 6(17):eaaz7822, 2020.

2. Lee CS, Hsu CY, Xu J, Sono T, Lee M, James A. Development of a biomaterial scaffold integrated with osteoinductive oxysterol liposomes to enhance hedgehog signaling and bone repair. *Molecular Pharmaceutics* 18(4):1677-1689, 2021.

3. Lee CS, Fan J, Hwang HS, Kim S, Chen C, Kang M, Aghaloo T, James A, Lee M. Bone-targeting exosome mimetics engineered by bioorthogonal surface functionalization for bone tissue engineering. [under review]

Books or other non-periodical, one-time publications.

Nothing to Report

Other publications, conference papers and presentations.

Nothing to Report

- **Website(s) or other Internet site(s)**

Nothing to Report

- **Technologies or techniques**

Nothing to Report

- **Inventions, patent applications, and/or licenses**

Nothing to Report

- **Other Products**

Nothing to Report

7. PARTICIPANTS & OTHER COLLABORATING ORGANIZATIONS

What individuals have worked on the project?

Name:	Min Lee
Project Role:	PI
Researcher Identifier	orcid.org/0000-0003-2813-2091
Nearest person month worked:	8
Contribution to Project:	Dr. Lee is responsible for the overall design and conduct of the project, oversight of all research activities, budget management, publication writing and scientific report preparation.
Funding Support:	NIH/NIDCR

Name:	Chung-Sung Lee
Project Role:	Postdoctoral Researcher
Researcher Identifier	orcid.org/0000-0001-5813-6056
Nearest person month worked:	28
Contribution to Project:	Dr. Lee has fabricated liposome and exosome nanocarriers, and also performed material characterization and data analysis
Funding Support:	N/A

Name:	Xiao Zhang
Project Role:	Postdoctoral Researcher
Researcher Identifier	orcid.org/0000-0002-0242-1939
Nearest person month worked:	12
Contribution to Project:	Dr. Zhang has performed the daily research and participated in the bioactivity test of drug-loaded liposomes as well as molecular biology analyses.

Funding Support:	N/A

Name:	Soyon Kim
Project Role:	Postdoctoral Researcher
Researcher Identifier	orcid.org/0000-0003-1030-8482
Nearest person month worked:	5
Contribution to Project:	Dr. Kim has performed material characterization and bioactivity test of liposomes.
Funding Support:	N/A

Name:	Minjee Kang
Project Role:	Postdoctoral Researcher
Researcher Identifier	orcid.org/0000-0002-0242-1939
Nearest person month worked:	10
Contribution to Project:	Dr. Kang participated in the preparation and characterization of exosomal delivery systems.
Funding Support:	N/A

Name:	Jiabing Fan
Project Role:	Project Scientist
Researcher Identifier	orcid.org/0000-0003-0285-0968
Nearest person month worked:	12
Contribution to Project:	Dr. Fan has performed the daily research and participated in the osteogenic activity test of drug-loaded exosomes as well as molecular biology analyses.
Funding Support:	N/A

Has there been a change in the active other support of the PD/PI(s) or senior/key personnel since the last reporting period?

Nothing to Report

What other organizations were involved as partners?

Johns Hopkins University

3400 N CHARLES ST
BALTIMORE MD 21218-2608

All *in vivo* studies and analyses were performed in the partner organization. The partner's research group has expertise in orthopaedic injury and analysis in murine models, as well as the manipulation of Hedgehog signaling during bone repair.

8. SPECIAL REPORTING REQUIREMENTS

COLLABORATIVE AWARDS:

Independent reports were submitted from the Initiating PI and Partnering PI.

QUAD CHARTS:

Not applicable

9. APPENDICES:

Award Chart

PR170115P1: Development of Smoothened Agonist Nonphospholipid Liposomal Nanoparticles for Bone Repair

PI: Min Lee, University of California, Los Angeles, CA
Topic Area: Nanomaterials for Bone Regeneration
Budget: $1,047,148
Mechanism: W81XWH-17-PRMRP-IIRA

0802, 0803, 0817, 0822

15 July 2018 – 14 July 2022

Study Goals:

To develop a nanoparticle delivered small molecule for faster, safer, and more efficacious bone repair than currently available treatment strategies

Specific Aims:

Aim 1: Optimize SAG-loaded liposomal nanoparticles for mouse calvarial defect repair
Aim 2: Determine the safety of SAG-loaded liposomal nanoparticles for mouse calvarial defect repair

Key Accomplishments and Outcomes:

Publications:

1. Lee CS, Kim S, Fan J, Hwang HS, Aghaloo T, Lee M. Smoothened Agonist Sterosome Immobilized Hybrid Scaffold for Bone Regeneration. *Science Advances* 6(17):eaaz7822, 2020.
2. Lee CS, Hsu CY, Xu J, Sono T, Lee M, James A. Development of a biomaterial scaffold integrated with osteoinductive oxysterol liposomes to enhance hedgehog signaling and bone repair. *Molecular Pharmaceutics* 18(4):1677-1689, 2021.
3. Lee CS, Fan J, Hwang HS, Kim S, Chen C, Kang M, Aghaloo T, James A, Lee M. Bone-targeting exosome mimetics engineered by bioorthogonal surface functionalization for bone tissue engineering. [under review]

Patents: N/A
Funding Obtained: N/A